

# CALIBRATION OF THE BEAM ENERGY POSITION MONITOR SYSTEM FOR THE RIKEN SUPERCONDUCTING ACCELERATION CAVITY

T. Watanabe\*, H. Imao, O. Kamigaito, N. Sakamoto, N. Fukunishi,  
M. Fujimaki, K. Yamada, Y. Watanabe, RIKEN, Wako, Japan

T. Toyama, T. Miyao, KEK/J-PARC, Tokai, Japan  
A. Miura, JAEA/J-PARC, Tokai, Japan

K. Hanamura, T. Kawachi, Mitsubishi Electric System & Service Co., Ltd., Tokai, Japan  
R. Koyama, SHI Accelerator Service Ltd., Wako, Japan  
A. Kamoshida, National Instruments Japan Corporation, Tokyo, Japan

## Abstract

Upgrades for the RIKEN Heavy-ion Linac that involve a new Superconducting Linac are currently underway to promote super-heavy element searches and radioactive isotope (RI) production of astatine ( $^{211}\text{At}$ ) for medical use. We have developed a beam energy position monitor (BEPM) system that can simultaneously measure not only the beam position but also the beam energy by measuring the time of flight of the beam. By using parabolic-shaped electrodes, we realized the ideal linear response of the quadrupole moments while maintaining good linear position sensitivity. We fabricated 11 BEPMs and the position calibration system employing a wire method that we used to obtain the sensitivity and offset of the BEPMs. Here, we present details concerning the BEPM system, calibration system, and measured results.

## INTRODUCTION

Nihonium is a synthetic super-heavy element that was discovered at RIKEN and is the first such element named by Japan. We aim to search for even heavier synthetic elements by using the upgraded Superconducting Linac (SRILAC) at the RIKEN RI Beam Factory (RIBF). Furthermore, the short-lived radio isotope  $^{211}\text{At}$ , which emits  $\alpha$  particles, attracts a lot of attention as a strong candidate for use in cancer therapy. Recently,  $^{211}\text{At}$  has been produced by using an  $\alpha$ -beam accelerated by the Azimuthally Varying Field (AVF) cyclotron at RIKEN [1,2]. The production rate of  $^{211}\text{At}$  increases with the energy of the  $\alpha$ -beam when the beam energy exceeds 22 MeV/u. However, production of polonium ( $^{210}\text{Po}$ ), which is very toxic to humans, starts to increase after the beam energy is raised above 30 MeV/u. Therefore, measuring and controlling the  $\alpha$ -beam energy are crucially important. An absolute accuracy of the beam energy measurement better than 0.1% should be achieved.

Destructive monitors generate outgassing; if they are used, it becomes difficult to maintain the Q value and surface resistance required to monitor the performance of the superconducting radio frequency (SRF) cavities over a long period of time. It is therefore crucial to develop nondestructive beam measurement diagnostics. With the aim to measure the beam position to an accuracy of  $\pm 0.1$  mm overall, a calibration measurement was performed at the KEK campus in Tokai.

## BEAM ENERGY AND POSITION MONITOR

The RIKEN Heavy-ion Linac (RILAC) at the present facility, and the beam transport lines and the SRILAC, which are under construction, are shown in Fig 1. Heavy-ion beams accelerated by the SRILAC are used by the GAs-filled Recoil Ion Separator (GARIS) III to search for super-heavy elements and to produce radioisotopes for medical use. If further acceleration is necessary, the beams are transported to the rear stage Riken Ring Cyclotron (RRC).

Here, depending on the installation location, 3 types of BEPM (Types I, II, and III) were designed and 11 BEPMs were fabricated [3] by Toyama Co., Ltd. [4]. BEPMs are installed in the center of the quadrupole magnets (Fig. 1), which are located between the SRF cavities. Photographs of the 3 types of BEPMs and a cross section of a BEPM are shown in Fig. 2, and the mechanical dimensions of each type of BEPM are summarized in Table 1.

By using a parabolic cut, the ideal linear response of the quadrupole moments is realized while maintaining a good linear position sensitivity [5]. The shape of an electrode is represented by  $y = (L/2) \cos 2\theta$ , where  $\theta$  is the angle in cylindrical coordinate system,  $y$  is the longitudinal axis, and  $L$  is the length of the electrode. During electrode processing, a mill cuts the end of the cylinder perpendicularly. Consequently, the edge plane of the electrode maintains a

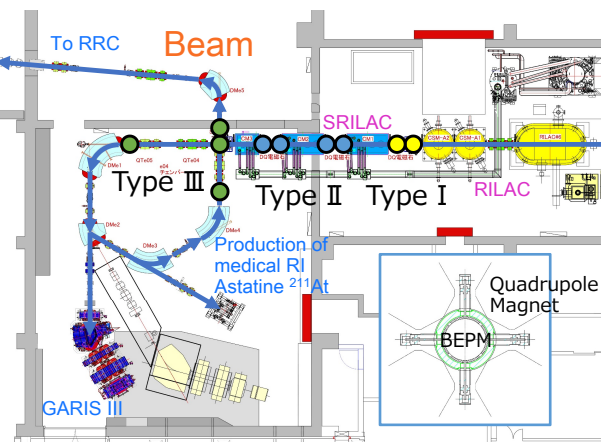


Figure 1: Schematic drawing of the RIKEN Heavy-ion Linac (RILAC), the upgraded Superconducting Linac (SRILAC), and the installation locations of the 3 types of BEPM.

\* wtamaki@riken.jp

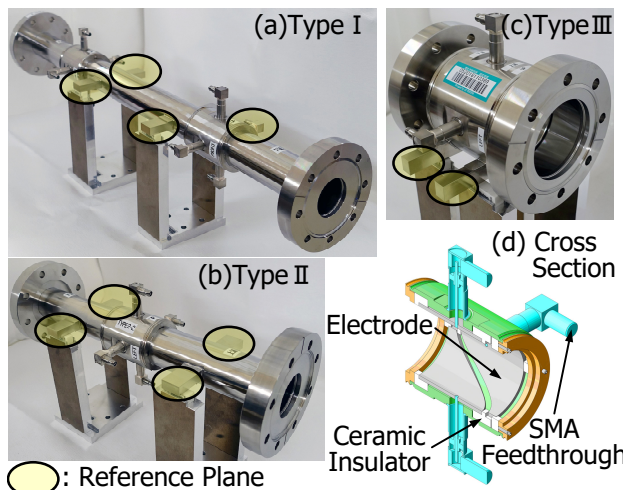


Figure 2: Photographs of the 3 types of BEPM: (a) Type I, (b) Type II, and (c) Type III. (d) Cross section drawing of a BEPM.

rectangular shape. Each BEPM has 4 reference planes in the  $x$ -axis direction and 8 in the  $y$ -axis direction; these reference planes are used for alignment and the calibration measurement. These reference planes are transferred from the center of the 4 electrodes, for which the mechanical accuracy is kept to within  $\pm 0.05$  mm, while that of the other parts is within  $\pm 0.1$  mm. Welding of the parts, including the vacuum flanges, tends to cause deformation. Therefore, after the welding process is completed, the reference planes are shaped again by using a milling cutter, and the mechanical accuracy is confirmed to be within the allowed values by using a 3-D coordinate measuring machine. The vacuum chamber, electrode, and flange are made of SUS316L, while the fixed and rotational flanges are made of ICF114. To electrically insulate between each electrode and the vacuum chamber, an alumina ceramic (AS999 [6]) is used, which has a low  $\tan\delta$  of  $0.5 \times 10^{-4}$  and a high purity of 99.99%. The signal induced on the electrode by the passing beam is sent outside the vacuum chamber via  $50 \Omega$  SMA feed-throughs [7].

Table 1: Mechanical Dimensions (mm) of 3 Types of BEPM

	Type I	Type II	Type III
Length of chamber	670	360	140
Outside dia. of chamber	58	58	85
Length of electrode	50	50	60
Inner dia. of electrode	40	40	60
Number of BEPMs	2	4	5

## CALIBRATION DEVICE AND JIGS

Calibration of the SRILAC BEPMs was carried out at the KEK Tokai campus by using a calibration device that was developed for the J-PARC Main Ring synchrotron [8, 9]. Because there are 3 types of BEPMs for the SRILAC, we designed and fabricated dummy pipes that surround the wire, and jigs to mechanically fit the calibration device.

### Precise Alignment

The calibration device is shown in Fig. 3. The BEPM to be measured is connected to a dummy pipe with inner diameter equal to that of one of the BEPMs (Fig. 3(a)). The assembly is fixed to an XY stage that moves within the measurement region at 2-mm step intervals. A wire acting as a signal source is fixed. Round crimp terminals are attached by crimping and soldering at both ends of a copper-plated piano wire. The dummy duct has a double-pipe structure that can be expanded and contracted. When the round crimp terminals are connected to the electrode on both end plates, the inner dummy pipes are made to slide into the outer dummy pipe to provide sufficient space for the connection of the electrodes. After that operation is completed, the inner dummy pipes are restored to their original position and fixed to the double pipe by fastening bands. Adequate tension can be applied by moving one of the end plates outward with a fine adjustment. The dummy pipes are connected to the end plates with an RF contact finger and are held to ground potential voltage (Fig. 3(b)). When the measurement was repeated, it was found that both the required electrical characteristics and flexibility could be achieved simultaneously by reducing the number of RF contact fingers and applying copper tape to the end panels. As a result, measurement errors were drastically reduced.

The calibration device has 2 reference coordinates in the  $x$ -axis direction (yellow squares) and 4 (blue squares) in the  $y$ -axis direction (Fig. 4). A gauge block (CERA block [10]) is fixed on the top of the calibration device's jig that supports the BEPM. The gauge block is used as a master gauge for precise measurement, with a mechanical error of less than  $0.1 \mu\text{m}$ . Although only 1 reference coordinate in the  $x$ -axis

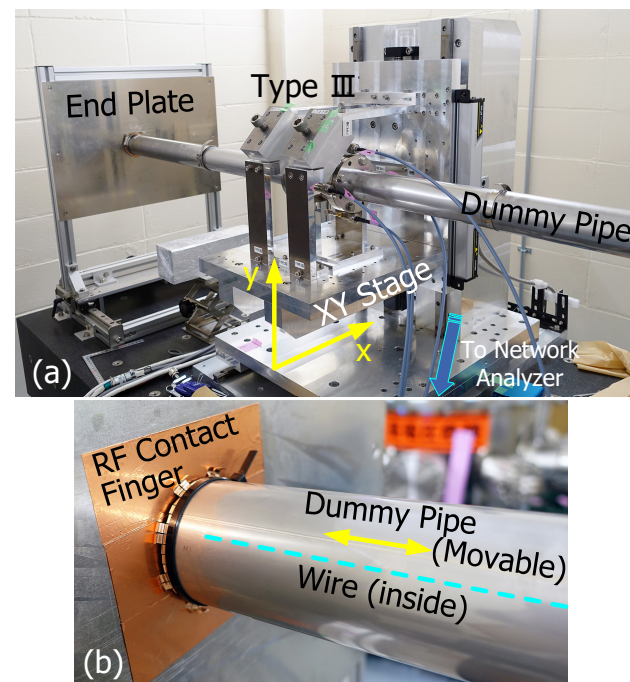


Figure 3: Photographs of the calibration measurement device, jigs, and dummy pipes.

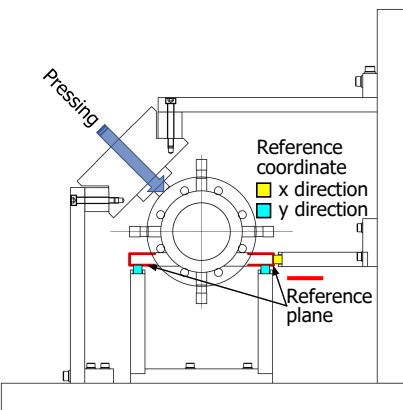


Figure 4: Reference planes and reference coordinates of the calibration device.

direction and 2 in the y-axis direction are shown in Fig. 4, an additional pair of reference coordinates is hidden behind. As mentioned above, the BEPM has 4 reference planes in the x-axis direction and 8 in the y-axis direction; these reference planes contact the reference coordinates of the calibration device.

The center position of the wire is measured by connecting the gauge block to the reference coordinate (Fig. 5). The total length of the gauge blocks is set equal to the distance between the center of the BEPM and the reference coordinate. Specifically, the wire is first made to touch the reference coordinate by moving the XY stage, after which the XY stage is moved at 1  $\mu\text{m}$  intervals to find the point where the wire no longer touches it; the continuity is monitored by current flow through the wire and gauge block. Finally, the radius of the wire is subtracted from this point to determine the center of the wire, namely the coordinate origin of the BEPM. This wire-fixing method has the following advantages: (1) there is no problem of wire wobbling, and (2) since the drive unit can be installed near the BEPM, stable operation can be obtained.

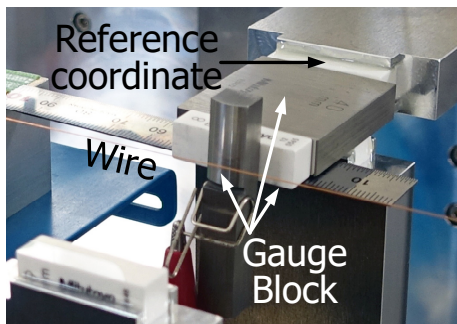


Figure 5: Measurement of the center position of the wire.

### Signal Processing System

A schematic drawing of the signal processing system is shown in Fig. 6. As mentioned above, the dummy duct has a double-pipe structure that can be expanded and contracted, and reflection of the signal is minimized by making the diameter of the dummy duct equal to that of the BEPM. A vector network analyzer (Rhode & Schwarz ZVT 8 [11]) is

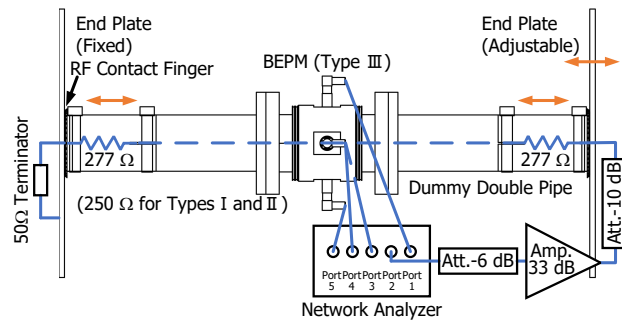


Figure 6: Schematic drawing of the signal processing system.

used to analyze the signal. The output signal from port 2 of the network analyzer (Fig. 6) is amplified by an amplifier (AA300-1S [12]) and fed into the input of the wire electrode. This signal is a sine wave, which takes the role of the simulated beam. The vector network analyzer measures the transmission coefficients from the wire to each electrode. 5-port TOSM (Through, Open, Short, Match) calibration of the vector network analyzer is carried out before the measurement. In addition, an attenuator is inserted before the amplifier to prevent damage to the amplifier due to reflection. The wire is 260  $\mu\text{m}$  in diameter ( $D_{in}$ ) and the inner diameters ( $D_{out}$ ) of each type of BEPM are listed in Table 1. If an insulator is the air, the characteristic impedance of a coaxial cable can be expressed as

$$Z_0 = 60 \Omega \log_e \frac{D_{out}}{D_{in}}. \quad (1)$$

From Eq. (1), the characteristic impedances are calculated as 302  $\Omega$  for Types I and II and 327  $\Omega$  for Type III. To minimize the wave reflected from the input signal, a 277- $\Omega$  resistor was inserted in series near both end plates for the Type III BEPM. Thus, the impedance seen by this BEPM is  $277 + 50 = 327 \Omega$ . Since this impedance is equal to what was calculated for Type III, the reflected wave nearly vanishes.

### Results of the Calibration Measurement

All 11 BEPMs were calibrated by using the calibration device. The temperature around the BEPM was set to 20°C, and if it deviated beyond  $20 \pm 1^\circ\text{C}$ , there was an error status alarm and forced termination. In addition, the same measurement was performed twice, and if the difference between the 2 results exceeded 50  $\mu\text{m}$ , the measurement was again repeated. By using the improved RF finger and copper tape setup described above, the measurement error was drastically reduced and converged within 50  $\mu\text{m}$ .

If the outputs from the 4 opposing right, left, up and down electrodes are represented by  $V_R$ ,  $V_L$ ,  $V_U$ , and  $V_D$ , respectively, the horizontal position  $x$  and the vertical position  $y$  of the wire are represented by the following relational expressions:

$$\begin{aligned} \frac{V_R - V_L}{V_R + V_L + V_U + V_D} &= \frac{\Delta_x}{\Sigma} = f_x(x, y) \approx k_x x, \\ \frac{V_U - V_D}{V_R + V_L + V_U + V_D} &= \frac{\Delta_y}{\Sigma} = f_y(x, y) \approx k_y y, \end{aligned} \quad (2)$$

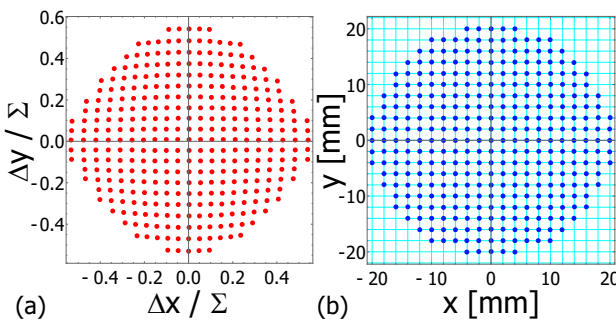


Figure 7: Results of the mapping measurement. (a) By using the electrode output voltages  $V_R$ ,  $V_L$ ,  $V_U$ , and  $V_D$ , the values of  $\Delta_x/\Sigma$  and  $\Delta_y/\Sigma$  are calculated and are plotted. (b) The results of the recalculation from the output of each electrode by using the calibration coefficients.

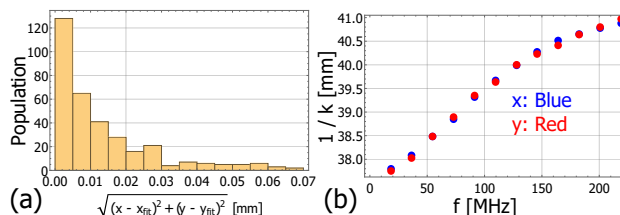


Figure 8: Results of the recalculation. (a) Residuals between the real wire position and the position obtained from the calibrated value. (b) Measured results of the inverse of the position sensitivity coefficients  $k$ , which are frequency dependent.

where  $f_x(x, y)$  and  $f_y(x, y)$  are 5<sup>th</sup>-order polynomial of the wire (or beam) and  $k$  is a position sensitivity coefficient. The 1<sup>st</sup> order approximations of  $f_x(x, y)$  and  $f_y(x, y)$  are  $k_x x$  and  $k_y y$ , respectively.

By using the electrode output voltages  $V_R$ ,  $V_L$ ,  $V_U$ , and  $V_D$ , the values of  $\Delta_x/\Sigma$  and  $\Delta_y/\Sigma$  are calculated using Eq. 2 and are plotted in Fig. 7(a). By fitting these measured data in Fig. 7(a) by a 5<sup>th</sup>-order polynomial,  $f_x(x, y)$  and  $f_y(x, y)$  were calculated, and the calibration coefficients were obtained.

Figure 7(b) shows the results of the recalculation from the output of each electrode by using the calibration coefficients. A histogram of the differences between the real wire position and the calculated position by using the calibration coefficients is shown in Fig. 8(a) the residuals are confirmed to be within 70  $\mu\text{m}$ . In addition, these calibration measurements were performed from 18.25 to 219 MHz in 12 steps of 18.25-MHz intervals. The inverse of the position sensitivity coefficients  $k$  of the BEPMs are frequency dependent, and the measured results are shown in Fig. 8(b). After completion of the calibration measurement, the capacitance of each electrode of each BEPM was also measured with the network analyzer.

## CONCLUSION

Calibration of the SRILAC BEPMs was carried out at the KEK Tokai campus by using a calibration device that

was developed for the J-PARC Main Ring synchrotron. For the 3 types of BEPMs, we designed and fabricated dummy pipes that surround the wire, and jigs to mechanically fit the calibration device. By using the calibration device, the calibration was completed to within  $\pm 0.05$  mm mechanical accuracy. We will continue to analyze the measurement results of all the BEPMs, which will be used to measure the beam position and energy using the calibration values when the beam is accelerated at SRILAC.

## ACKNOWLEDGEMENTS

The authors thank Y. Ohnishi at Toyama Co., Ltd., for providing CAD data for the BEPM, the jigs, and the dummy pipes.

## REFERENCES

- [1] N. Sato *et al.*, “Development of a production technology of 211At at the RIKEN AVF cyclotron: (i) Production of 211At in the 209Bi( $\alpha, 2n$ )211At reaction”, RIKEN Accel. Prog. Rep. 50, p. 262 (2017).
- [2] S. Yano *et al.*, “Development of a production technology of 211At at the RIKEN AVF cyclotron: (ii) Purification of 211At by a dry distillation method”, RIKEN Accel. Prog. Rep. 50, p. 263 (2017).
- [3] T. Watanabe *et al.*, “Developement of Beam Energy Position Monitor System for Riken Superconducting Acceleration Cavity”, in *Proceedings of the 15th Annual Meeting of Particle Accelerator Society of Japan*, Nagaoka, Japan, Aug. 2018, pp. 49-54, paper WEOL09. <http://www.pasj.jp/web-publish/pasj2018/proceedings/index.html>
- [4] <http://www.toyama-en.com/>
- [5] G. Nassibian, “The Measurement of the Multipole Coefficients of a Cylindrical Charge Distribution”, CERN/SI/Note EL/70-13 (1970).
- [6] <http://www.ft-ceramics.co.jp/eng/>
- [7] <https://www.maruwa-g.com/e/>
- [8] K. Hanamura *et al.*, “Development of Calibration System for Bpm at J-Parc 50 GeV Synchrotron”, in *Proceedings of the 3rd Annual Meeting of the Particle Accelerator Society of Japan and the 31th Linear Accelerator Meeting in Japan*, Sendai, Japan, Aug. 2006, pp. 466-468; [http://www.pasj.jp/web\\_publish/pasj3\\_lam31/Proceedings/W/WP66.pdf](http://www.pasj.jp/web_publish/pasj3_lam31/Proceedings/W/WP66.pdf)
- [9] T. Miura *et al.*, “Calibration of Beam Position Monitor for J-PARC Main Ring Synchrotron”, in *Proceedings of the 3rd Annual Meeting of the Particle Accelerator Society of Japan and the 31th Linear Accelerator Meeting in Japan*, Sendai, Japan, Aug. 2006, pp. 469-471; [http://www.pasj.jp/web\\_publish/pasj3\\_lam31/Proceedings/Proceedings/W/WP67.pdf](http://www.pasj.jp/web_publish/pasj3_lam31/Proceedings/Proceedings/W/WP67.pdf)
- [10] <https://www.mitutoyo.co.jp/eng/>
- [11] [https://www.rohde-schwarz.com/home\\_48230.html](https://www.rohde-schwarz.com/home_48230.html)
- [12] <http://www.rk-microwave.com/index.php>